Journal of Molecular Medicine (2019) 97:1247–1261
https://doi.org/10.1007/s00109-019-01813-w

JMolMed

ORIGINAL ARTICLE

Preclinical studies of a death receptor 5 fusion protein that ameliorates acute liver failure

Qian Chen[1,2] · Pu Wang[1] · Qingmei Zhang[3] · Meng Xia[3] · Guizhong Zhang[1] · Junxin Li[1,2] · Enyun Shen[3] · Youhai H. Chen[4] · Xiaochun Wan[1,5]

Received: 3 November 2018 / Revised: 10 June 2019 / Accepted: 14 June 2019 / Published online: 22 June 2019

Abstract

Acute liver failure (ALF) is a life-threatening disease with a high mortality rate. There is an urgent need to develop new drugs with high efficacy and low toxicity. In this study, we produced a pharmaceutical-grade soluble death receptor 5 (sDR5)-Fc fusion protein for treating ALF and evaluated the pharmacology, safety, pharmacokinetics, efficacy, and mechanisms of sDR5-Fc in mice, rats, and cynomolgus monkeys. sDR5-Fc bound with high affinity to both human and monkey tumor necrosis factor-related apoptosis-inducing ligand (TRAIL) effectively blocked TRAIL-induced apoptosis in vitro and significantly ameliorated ALF induced by concanavalin A (Con A) in mice. Mechanistically, sDR5-Fc inhibited hepatocyte death and reduced inflammation in vivo. Furthermore, sDR5-Fc attenuated the production of inflammatory cytokines by splenocytes activated with Con A or an anti-CD3 antibody in vitro. Consistent with these results, splenocytes from $TRAIL^{-/-}$ mice produced much lower levels of inflammatory cytokines than those from $TRAIL^{+/+}$ mice. In cynomolgus monkeys, sDR5-Fc was safe and well tolerated when intravenously administered as a single dose of up to 1200 mg/kg or multiple doses of 100 mg/kg. After treatment with a single dose, linear pharmacokinetics with a mean half-life of > 1.9 days were observed. After 12 weekly doses, sDR5-Fc exposure increased in an approximately dose-proportional manner, and the mean accumulation ratio ranged from 1.82- to 2.11-fold. These results support further clinical development of our sDR5-Fc protein as the first TRAIL-targeting drug for ALF treatment.

Key messages

- sDR5-Fc binds with high affinity to TRAIL to effectively block TRAIL-induced apoptosis.
- sDR5-Fc ameliorates Con A-induced acute liver failure in mice by inhibiting hepatocyte death and inflammation.
- sDR5-Fc or TRAIL knockout attenuates the production of inflammatory cytokines by activated splenocytes in vitro.
- sDR5-Fc is safe and well tolerated in acute or long-term toxicity study.

Keywords Acute liver failure · Death receptor · TRAIL · Inflammation · Apoptosis

Electronic supplementary material The online version of this article (https://doi.org/10.1007/s00109-019-01813-w) contains supplementary material, which is available to authorized users.

✉ Youhai H. Chen
yhc@pennmedicine.upenn.edu

✉ Xiaochun Wan
xc.wan@siat.ac.cn

[1] Shenzhen Laboratory of Antibody Engineering, Institute of Biomedicine and Biotechnology, Shenzhen Institutes of Advanced Technology, Chinese Academy of Sciences, Shenzhen 518055, China

[2] University of Chinese Academy of Sciences, Beijing 100049, China

[3] Shenzhen Zhongke Amshenn Pharmaceutical Co., Shenzhen 518055, China

[4] Department of Pathology and Laboratory Medicine, Perelman School of Medicine, University of Pennsylvania, Philadelphia, PA 19104, USA

[5] Shenzhen BinDeBioTech Co., Shenzhen 518055, China

Introduction

Acute liver failure (ALF), also termed fulminant hepatic failure, is a life-threatening illness [1]. To date, limited therapeutic approaches are available to treat ALF, and the mortality rate of ALF can be as high as 50% [2]. Therefore, there is a strong unmet need to develop new drugs for ALF treatment.

Apoptosis is an important cellular process that is essential for maintaining physiological homeostasis. Dysregulation of hepatocyte apoptosis is a common molecular mechanism that underlies a large number of liver diseases such as viral hepatitis, fatty liver, hepatic fibrosis, and ALF [3]. Death receptor 4 and death receptor 5 (DR4 and DR5), also known as tumor necrosis factor (TNF)-related apoptosis-inducing ligand (TRAIL) receptor-1 and receptor-2, are important initiators of hepatocyte apoptosis [4]. Previous studies showed that the expression level of TRAIL is much higher in hepatitis B or C virus (HBV or HCV)-infected patients than in healthy controls [5–10], and DR5 expression is upregulated in patients with nonalcoholic steatohepatitis [11] or cholestasis [12]. Therefore, TRAIL-mediated hepatocyte apoptosis may play an important role in hepatic injury in a variety of medical conditions, including viral infections, autoimmune diseases, and metabolic disorders [9, 13, 14], and TRAIL is a promising therapeutic target for treating these diseases.

DR5 is a member of the TNF receptor superfamily. The naturally occurring molecule soluble DR5 (sDR5) lacks the transmembrane and intracellular regions of DR5 and is therefore capable of blocking the activity of TRAIL [15]. Blocking endogenous TRAIL with sDR5 can enhance the proliferation of autoreactive lymphocytes or synovial cells and lead to exacerbated collagen-induced arthritis [16]. On the other hand, a recombinant adenovirus that produces a soluble DR5-Fc fusion protein has been shown to prevent TRAIL-mediated hepatocyte apoptosis and decrease the production of IFN-γ and TNF-α [17]. TRAIL-deficient mice are resistant to concanavalin A (Con A)- and *Listeria*-induced hepatitis [18]. The injection of purified sDR5 produced by *Pichia pastoris* 24 h before the onset of acute murine hepatitis induced by HBV-containing plasmids significantly alleviates liver damage [19].

However, sDR5 is unstable with a short half-life. Therefore, we produced a pharmaceutical-grade recombinant sDR5-Fc fusion protein, which consisted of the extracellular ligand-binding domain of human DR5 and the Fc portion of human immunoglobulin G1 (IgG1). We describe below the preclinical characterizations of this fusion protein as well as mechanisms underlying its therapeutic effect on a model of ALF. The data suggest that sDR5-Fc, the first TRAIL-blocking drug, holds great promise for clinical development because of its high efficacy and low toxicity.

Methods

Production of a pharmaceutical-grade recombinant DR5 fusion protein

The cDNA sequences coding for the leader and extracellular domain of human DR5 and the Fc portion of human IgG1 including the CH_2 and CH_3 domains were amplified by PCR and cloned into the eukaryotic expression vector pL101, which contains an hCMV promoter and a glutamine synthetase gene (Zhangjiang Biotechnology Co., Shanghai, China). pL101-DR5-Fc was transfected into CHO-K1 cells by electroporation. Several recombinant CHO-K1 cell clones secreted a large amount of sDR5-Fc, reaching up to 1.2 g/L of cell culture. sDR5-Fc was purified by affinity chromatography; depleted of endotoxins, host proteins, DNAs, and microorganisms by ultrafiltration; and stored at −80 °C. The sDR5-Fc protein was sterile, the level of endotoxins was below 0.50 EU/mg, and the purity was over 99% when analyzed by size exclusion-high-performance liquid chromatography (SEC-HPLC). The molecular weight of sDR5-Fc was identified by high-resolution mass spectrometry.

Surface plasmon resonance analysis

Surface plasmon resonance (SPR) experiments were carried out with a BIAcore 8k (GE Healthcare, Uppsala, Sweden) using immobilized purified sDR5-Fc protein on a BIAcore CM5 sensor chip. The immobilization of sDR5-Fc was performed at 25 °C, and HBS-EP$^+$ (10 mM HEPES, 150 mM NaCl, 3 mM EDTA, and 0.05% P20, pH 7.4) was used as the running buffer. Briefly, both flow cells of channel 2 of the sensor chip were activated by freshly mixed 50 mmol/L N-hydroxysuccinimide and 200 mmol/L 1-ethyl-3-(3-dimethylaminopropyl) carbodiimide hydrochloride for 300 s (10 μL/min). Then, 2 μg/mL sDR5-Fc diluted in 10 mmol/L NaAC (pH 4.0) was injected into the flow cell 2 to reach a level of approximately 100 units of response, while flow cell 1 was set as the blank. After the amine coupling reaction, the remaining active coupling sites were blocked with a 300-s injection of 1 mol/L ethanolamine hydrochloride. The measurement was performed at 25 °C, and HBS-EP$^+$ was used as the running buffer. An injection of the tested analyte and surface regeneration of the CM5 sensor chip were included in each running cycle. Serially diluted TRAIL proteins (human TRAIL 0, 0.3125, 0.625, 1.25, 2.5, 5, and 10 nM; rhesus monkey TRAIL 0, 0.3125, 0.625, 1.25, 2.5, 5, and 10 nM; and mouse TRAIL 25, 50, 100, 200, 400, and 800 nM) were injected sequentially into both cells of channel 2 (30 μL/min) with an association time of 180 s, and buffer flow was maintained for 600 s for dissociation. The TRAIL proteins were purchased from Sino Biological Inc. (10409-HNAE, 90098-CNAE, and 50166-M07E; Beijing, China). To remove the

tested proteins for regeneration, a duplicate 30-s injection of 10 mM glycine-HCl (pH 1.5) was used. K_D values were calculated with BIAcore 8k evaluation software 1.0 with a 1:1 binding model.

Neutralization assay

L929 and HepG2 cells were cultured in DMEM (SH30021.01, HyClone, Logan, USA), and Jurkat cells were cultured in RPMI 1640 medium (SH30809.01, HyClone). All cell lines were purchased from the Cell Bank of the Chinese Academy of Sciences (Shanghai, China), maintained in medium containing 10% FBS (SH30084.03, HyClone) and 1% penicillin-streptomycin (SV30010, HyClone), and incubated at 37 °C with 5% CO_2. Cells were harvested and diluted to 8×10^4 cells/mL, added to 96-well plates (100 μL per well), and then incubated for 24 h. sDR5-Fc was prepared in 2-fold dilutions, and each diluted sample was mixed with an equal volume of human TRAIL (375-TEC-010, R&D systems, Minneapolis, MN, USA) and actinomycin D (A8030, Shanghai Biolight, Shanghai, China). The concentrations of TRAIL were 4 ng/mL, 3.5 ng/mL, and 3 ng/mL for the L929, HepG2, and Jurkat cells, respectively. The concentration of actinomycin D was 5 μg/mL for the L929 cells and 0.5 μg/mL for the HepG2 and Jurkat cells. After 20 h of culture, the reagent mixture (MTS/PMS, G5430, Promega, Madison, WI, USA) was added to each well. Three hours later, the absorbance was measured at 490 nm with a reference wavelength of 630 nm using an enzyme-linked immunosorbent assay (ELISA) reader (Multiskan Go, ThermoFisher, Waltham, MA, USA).

Preclinical safety and pharmacokinetic studies

Good laboratory practice (GLP) studies were conducted by JOINN Laboratories, Inc. (Suzhou, China), including the acute toxicity study, long-term toxicity study, biodistribution study, and pharmacokinetic study. The detailed methods are provided in the Supplementary Materials.

Animal studies

Six- to eight-week-old male C57BL/6J mice (weight 18–25 g) were purchased from Hunan SJA Laboratory Animal Co. (Hunan, China). All animal care and experimental studies were approved by the *Institutional Animal Care and Use Committee* (IACUC) of Shenzhen Institutes of Advanced Technology, Chinese Academy of Sciences. Animal studies adhered to the ARRIVE guidelines [20, 21]. Mice were kept in standard individually ventilated cages in an animal facility under standardized conditions (12-h light/dark cycle, 18–25 °C, and 50–60% humidity) with food and water provided ad libitum. All efforts were made to minimize the suffering of the animals and the number of animals needed to obtain reliable results.

We chose the Con A-induced liver failure mouse model because it is a well-established experimental model that mimics the symptoms and pathological progression of human ALF [22–25]. Mice were assigned randomly into four groups ($n = 6$–10 per group): vehicle only, sDR5-Fc only, Con A + vehicle, and Con A + sDR5-Fc. Mice were injected intravenously (i.v.) with Con A (L7647, Sigma-Aldrich, St. Louis, MO, USA) or left untreated, and 1 h later, the mice were i.v. administered sDR5-Fc or the vehicle. Normal pyrogen-free saline (G15092203, Guangdong Kelun Pharmaceutical Co., Meizhou, China) was used as a vehicle control. The survival rate was monitored. At 8 or 24 h post-Con A injection, peripheral blood, liver, and spleen samples were collected for analyses of serum biochemistry indexes, cytokines, and pathological histology or used to isolate mononuclear cells and RNA transcripts.

The blood samples were centrifuged at 3000 × rpm for 10 min at 4 °C to isolate the serum. Serum alanine aminotransferase (ALT), aspartate aminotransferase (AST), lactate dehydrogenase (LDH), and total bile acid (TBA) levels were measured by the standard photometric method using an automatic analyzer (BS-180, Mindray, Shenzhen, China). Serum IL-6, IFN-γ, TNF-α, and IL-2 levels were measured with a mouse Th1/Th2/Th17 cytometric bead array (CBA) kit (560485, BD Biosciences, San Jose, CA, USA), and the serum sTRAIL level was measured with a mouse TRAIL ELISA kit (ab193730, Abcam, Cambridge, MA, USA).

$TRAIL^{-/-}$ mice were generated as previously described [26]. Control $TRAIL^{+/+}$ mice were purchased from The Jackson Laboratory (Bar Harbor, Maine, USA). Mice were housed in the University of Pennsylvania animal facilities under pathogen-free conditions. All animal protocols involving $TRAIL^{-/-}$ mice were preapproved by the IACUC at the University of Pennsylvania. Seven- to eight-week-old male mice ($n = 5$ per group, weight 20–25 g) were injected i.v. with 25 mg/kg Con A. Blood was obtained, and serum IL-6, IFN-γ, TNF-α, and IL-12 levels were measured by ELISA (BD).

HE staining, TUNEL assay, and immunohistochemistry

Liver tissue was washed with PBS, fixed in 4% buffered paraformaldehyde, embedded in paraffin, and sectioned. The slides were stained with hematoxylin and eosin (HE) and viewed under a light microscope. Twelve fields for each condition were randomly acquired at × 200 magnification. The sections were also used to detect nuclear DNA strand breaks using an in situ apoptosis detection kit (G3250, Promega) according to the manufacturer's protocols. The apoptotic ratio in the liver was calculated as follows: the number of TUNEL-

positive cells divided by the total number of stained nuclei. Six fields were analyzed for each section, and an average number of three sections were evaluated for each group. Images were acquired under a fluorescence microscope (BX53, Olympus, Tokyo, Japan) with a CCD camera (DP80, Olympus).

Tissue sections were dewaxed, rehydrated through graded ethanol dilutions, and then heated in a citrate buffer (pH 6, 10 mM) in a microwave oven at 100 °C for 20 min. Endogenous peroxidase activity was blocked with 3% hydrogen peroxide followed by washing. The sections were then incubated with an anti-TRAIL antibody (sc-6079, Santa Cruz Biotechnology, Santa Cruz, CA, USA). A horseradish peroxidase (HRP)-conjugated rabbit anti-goat secondary antibody (5220-0362, SeraCare KPL, Milford, MA, USA) was used according to the manufacturer's instructions. Histochemical development was achieved with a commercial 3,3′-diaminobenzidine (DAB) substrate kit (SK-4105, Vector Laboratories, Burlingame, CA, USA). All sections were counterstained with hematoxylin and were visualized using an Olympus microscope.

Flow cytometry

Mononuclear cells were prepared from the liver, spleen, and peripheral blood as described previously [27, 28]. The cells were stained with fluorescently labeled antibodies to identify surface antigens. The antibodies used are listed in Supplementary Table S1. A live/dead fixable violet dead cell stain kit (L34963, Life Technologies, Carlsbad, CA, USA) or 7-AAD (420403, BioLegend, San Diego, CA, USA) was used to exclude dead cells. CountBright absolute counting beads (C36950, Life Technologies) were added to determine the cell number. The stained cells were analyzed using a high-performance flow cytometer (FACSCanto II, BD Biosciences), and the data were analyzed with FlowJo software.

RNA isolation and real-time quantitative PCR

Total RNA was extracted with TRIzol (15596018, Invitrogen, Carlsbad, CA, USA) according to the manufacturer's instructions. Real-time quantitative RT-PCR analysis was performed using the specific primers listed in Supplementary Table S2 in an Applied Biosystems 7500 system with a StarScript II green fast one-step qRT-PCR kit (A323, Genstar, Beijing, China). Using GAPDH as the control, relative expression was calculated by using the comparative Ct method and expressed as the fold change (2-ΔΔCt) as previously described [29].

Splenocyte stimulation

Mouse splenocytes were isolated and stimulated with Con A (5 μg/mL) or anti-CD3 antibody (1 μg/mL, 100202, BioLegend) for 3 days. sDR5-Fc was added to evaluate its effects on lymphocyte activation and inflammatory cytokine secretion. The culture supernatants were collected for cytokine concentration detection, and the cells were harvested for cytokine mRNA detection or Western blot analysis.

Mouse splenocytes isolated from $TRAIL^{-/-}$ and $TRAIL^{+/+}$ mice were stimulated with Con A or the anti-CD3 antibody. The cells were cultured for 3 days with [3H]-thymidine for the last 16 h. The plates were harvested, and the level of radioactivity (presented as cpm) was determined using a Wallac β-plate counter.

The following methods are described in the Supplementary Materials and Methods: immunoblotting, blocking specificity of sDR5-Fc for TRAIL, and a binding affinity assay.

Data and statistical analysis

All data are expressed as the mean ± standard deviation (SD) or standard error (SEM). All statistical analyses were performed using GraphPad Prism 6 (GraphPad Software Inc., San Diego, CA, USA). Differences among the experimental groups were determined by an unpaired Student's *t* test or one-way ANOVA. For survival analysis, the log-rank (Mantel-Cox) test was used to compare groups. All the non-GLP experiments were performed a minimum of three times. $*P < 0.05$ was considered to show statistical significance. "ns" indicates a difference was not significant ($P > 0.05$).

Results

Characterization of a recombinant sDR5-Fc fusion protein

A schematic representation of recombinant sDR5-Fc is shown in Fig. 1a. The sDR5-Fc protein purified from CHO-K1 cells ran as a single Coomassie-stained band on a nonreducing SDS-PAGE gel with an apparent molecular mass of 79.4 kDa (Fig. 1b, Supplementary Fig. S1a). However, the monomer molecular mass found by matrix-assisted laser desorption/ionization mass spectrometry was 39.7 kDa (Supplementary Fig. S1b), which was larger than the molecular weight predicted from the amino acid sequence (38.3 kDa) and suggested that the protein was glycosylated. The purity of sDR5-Fc was over 99% by SEC-HPLC (Fig. 1c). We characterized the affinity of sDR5-Fc binding to TRAIL proteins from different species by SPR (Fig. 1d, Table 1). The binding affinity of sDR5-Fc for human TRAIL was comparable to that of sDR5-Fc for rhesus monkey

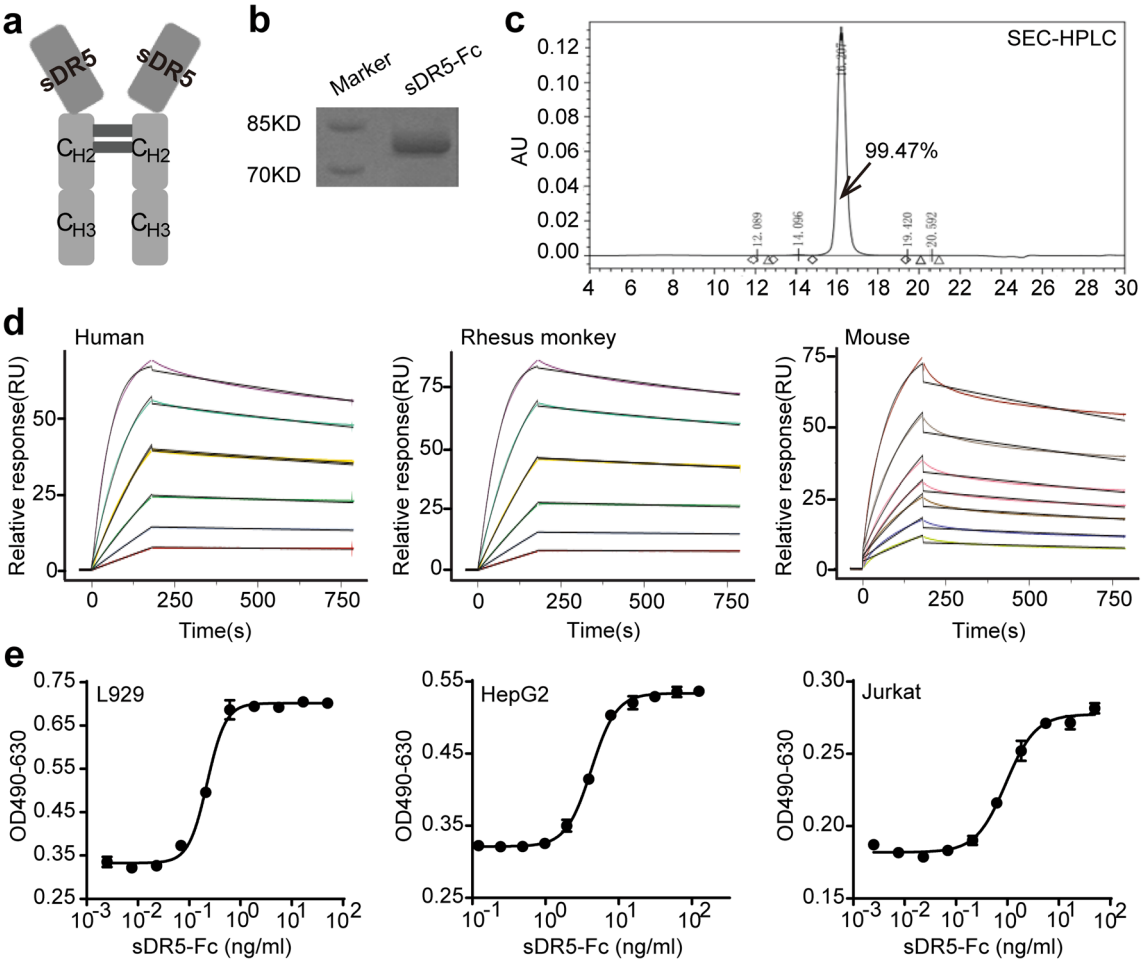

Fig. 1 Characterization of the recombinant sDR5-Fc fusion protein. **a** A schematic representation of the molecular structure of the sDR5-Fc fusion protein. **b** Coomassie-stained SDS-PAGE gel showing the sDR5-Fc protein after purification. **c** A SEC-HPLC chromatogram of the purified sDR5-Fc protein. **d** SPR analyses of sDR5-Fc binding to human, rhesus monkey, or mouse TRAIL protein. Normalized sensorgrams using the sDR5-Fc protein as the ligand and the TRAIL protein as the analyte are shown. The concentrations of human and monkey TRAIL included 0.3125, 0.625, 1.25, 2.5, 5, and 10 nM. The concentrations of mouse TRAIL included 25, 50, 100, 200, 400, and 800 nM. The raw data (colored lines) were fitted to a 1:1 binding model (black lines). **e** MTT analysis of the effect of sDR5-Fc on TRAIL-induced apoptosis in L929, HepG2, and Jurkat cells. Data are expressed as the mean ± SEM for duplicated measures. Data are representative of 3 independent experiments

TRAIL and was significantly stronger than that of sDR5-Fc for mouse TRAIL.

To test the ability of sDR5-Fc to block human TRAIL signaling, L929, HepG2, and Jurkat cells were treated with a recombinant human TRAIL protein in the presence or absence of sDR5-Fc. The human TRAIL protein exhibited significant cytotoxicity within 24 h (Supplementary Fig. S1c-e), and sDR5-Fc demonstrated a dose-dependent inhibitory effect on TRAIL-induced apoptosis (Fig. 1e). The EC_{50} values of sDR5-Fc in L929, HepG2, and Jurkat cells were 0.22 ng/mL, 4.0 ng/mL, and 0.95 ng/mL, respectively. In addition to interacting with TRAIL, sDR5 can interact with membrane-bound DR5 [30]. We did not clearly detect binding interactions between sDR5-Fc (at 100 μg/mL) and membrane-bound DR5 in L929 or HepG2 cells by flow cytometry (Supplementary Fig. S2a-c). sDR5-Fc was found to bind to Jurkat cells in a dose-dependent manner, however, through the Fc receptor expressed on the membrane of Jurkat cells (Supplementary Fig. S2d). The binding affinities of sDR5-Fc for human TRAIL and sDR5 were determined by the ForteBio Octet System (Supplementary Fig. S2e-f). TRAIL (12.5–100 nM) efficiently bound to sDR5-Fc in a concentration-dependent manner; however, a binding interaction between sDR5 (up to 800 nM) and sDR5-Fc was not observed. Altogether, these results indicated that sDR5-Fc had high activity in blocking TRAIL-induced apoptosis.

sDR5-Fc protects against Con A-induced ALF

To examine the therapeutic potential of sDR5-Fc in vivo, mice were challenged with a lethal dose of Con A (17 mg/kg) and then treated with sDR5-Fc (10–30 mg/kg) or vehicle 1 h later.

Table 1 The affinity and kinetics data of the binding of TRAIL proteins of different species to sDR5-Fc

Ligand	Analyte	k_a (1/Ms)	k_d (1/s)	K_D (M)	Chi^2 (RU^2)
sDR5-Fc	Human TRAIL	2.91E + 06	3.01E − 04	1.03E − 10	2.24E − 01
	Rhesus TRAIL	2.89E + 06	2.63E − 04	9.12E − 11	1.88E − 01
	Mouse TRAIL	1.73E + 04	3.83E − 04	2.22E − 08	7.02E − 01

All mice in the vehicle group died within 6 days of the Con A injection. In contrast, 37.5% of the mice in the 30 mg/kg sDR5-Fc group survived for more than 30 days after the Con A injection ($P < 0.01$, Fig. 2a). Treatment with 10 mg/kg or 20 mg/kg sDR5-Fc also significantly increased mouse survival ($P < 0.05$, Fig. 2a). The effect of sDR5-Fc on hepatic damage was determined in mice preinjected with a sublethal dose of Con A. Con A (9 mg/kg) caused significant increases in the serum levels of ALT, AST, LDH, and TBA. Treatment with sDR5-Fc significantly decreased the levels of the serum liver function indicators elevated by Con A (Fig. 2b). Histological examination of HE-stained liver sections revealed inflammatory cell infiltration and widespread hepatocyte death induced by Con A (Fig. 2c, e). sDR5-Fc administration at 1 h after Con A challenge significantly attenuated liver injury, as evidenced by a reduction in the hepatic injury area. Additionally, sDR5-Fc significantly reduced the number of apoptotic cells, determined by TUNEL staining (Fig. 2d, f). Taken together, these results showed that sDR5-Fc effectively protected against Con A-induced ALF.

sDR5-Fc attenuates inflammation induced by Con A

Lymphoid and myeloid cells of the immune system are the initiators and effectors of Con A-induced hepatitis [31, 32]. To investigate the effect of sDR5-Fc on these leukocytes in Con A-treated mice, we isolated mononuclear cells from the liver, spleen, and peripheral blood and analyzed them by flow cytometry. We found that 9 mg/kg Con A significantly increased the number of inflammatory cells in the liver at 8 h after injection, and 9 mg/kg sDR5-Fc therapy significantly attenuated the infiltration of leukocytes (Fig. 3a, Supplementary Fig. S3a). Using T, B, and NK cell markers, several distinct subsets of lymphocytes were identified. sDR5-Fc therapy reduced the numbers of T cells, including $CD4^+$ T, $CD8^+$ T, and $CD4^-CD8^-$ T cells (Fig. 3a, Supplementary Fig. S3b-d). Using the markers CD11b, Gr1, Ly6C, Ly6G, and F4/80, we observed that Con A significantly induced the accumulation of $CD11b^+$ cells, especially $CD11b^+Gr1^+$ cells expressing both Ly6G and Ly6C, in the liver, which was consistent with previous studies [32]. sDR5-Fc therapy had no significant effect on the numbers of $CD11b^+$ subset cells (Supplementary Fig. S3e). In contrast, in the peripheral blood and spleen, the number of leukocytes was significantly reduced by Con A injection (Supplementary Fig. S4). sDR5-Fc therapy significantly increased the number of leukocytes in the peripheral blood, but had no effect on the number of splenocytes. Taken together, these results showed that sDR5-Fc effectively attenuated the infiltration of leukocytes into the liver induced by Con A and markedly normalized the number of leukocytes in the peripheral blood.

By immunohistochemistry, we observed abundant $TRAIL^+$ cells in the severely damaged liver tissue of Con A-treated mice (Fig. 3b). The number of these $TRAIL^+$ cells was markedly reduced by sDR5-Fc therapy (Fig. 3c). In addition to its effect on the infiltration of inflammatory cells, sDR5-Fc significantly reduced inflammatory cytokine levels in the serum (Fig. 3d) and the mRNA expression of *Il6*, *Ifng*, *Tnfa*, *Il2*, and *Il1b* in the liver (Fig. 3e) in Con A-challenged mice. Likewise, the mRNA expression levels of *Trail* and *Dr5* increased in the liver following Con A injection but were significantly attenuated by sDR5-Fc treatment (Fig. 3e).

sDR5-Fc inhibits the production of inflammatory mediators by attenuating NF-κB activation

Con A is a strong mitogen for leukocytes including T lymphocytes. By using a methylthiazolyldiphenyl-tetrazolium bromide (MTT) assay, we detected the effect of sDR5-Fc on the Con A-dependent proliferation of mouse splenocytes in vitro. sDR5-Fc did not affect the proliferation of splenocytes (Supplementary Fig. S5), but significantly reduced the IL-6, IFN-γ, TNF-α, and IL-2 levels in culture supernatants of Con A-stimulated splenocytes as well as the mRNA levels of *Il6*, *Ifng*, *Tnfa*, and *Trail* in splenocytes (Fig. 4a, b). Similarly, sDR5-Fc also significantly inhibited the production of these cytokines by splenocytes stimulated with an anti-CD3 antibody in a dose-dependent manner (Fig. 4c). The transcription factor NF-κB plays an important role in the inflammatory response. Activation of the inflammatory pathway controlled by NF-κB is one of the first reported non-canonical signals elicited by TRAIL. Using phosphorylated p65 (p-p65) as a surrogate marker for NF-κB activity, we found that sDR5-Fc treatment decreased the p-p65 level in a dose-dependent manner in Con A-activated splenocytes (Fig. 4d). There were no significant effects on the levels of p65, c-Rel, p100/p52, or phosphorylated-p38. Thus, by attenuating NF-κB activation, blocking TRAIL with sDR5-Fc inhibits the production of inflammatory mediators by splenocytes activated in vitro.

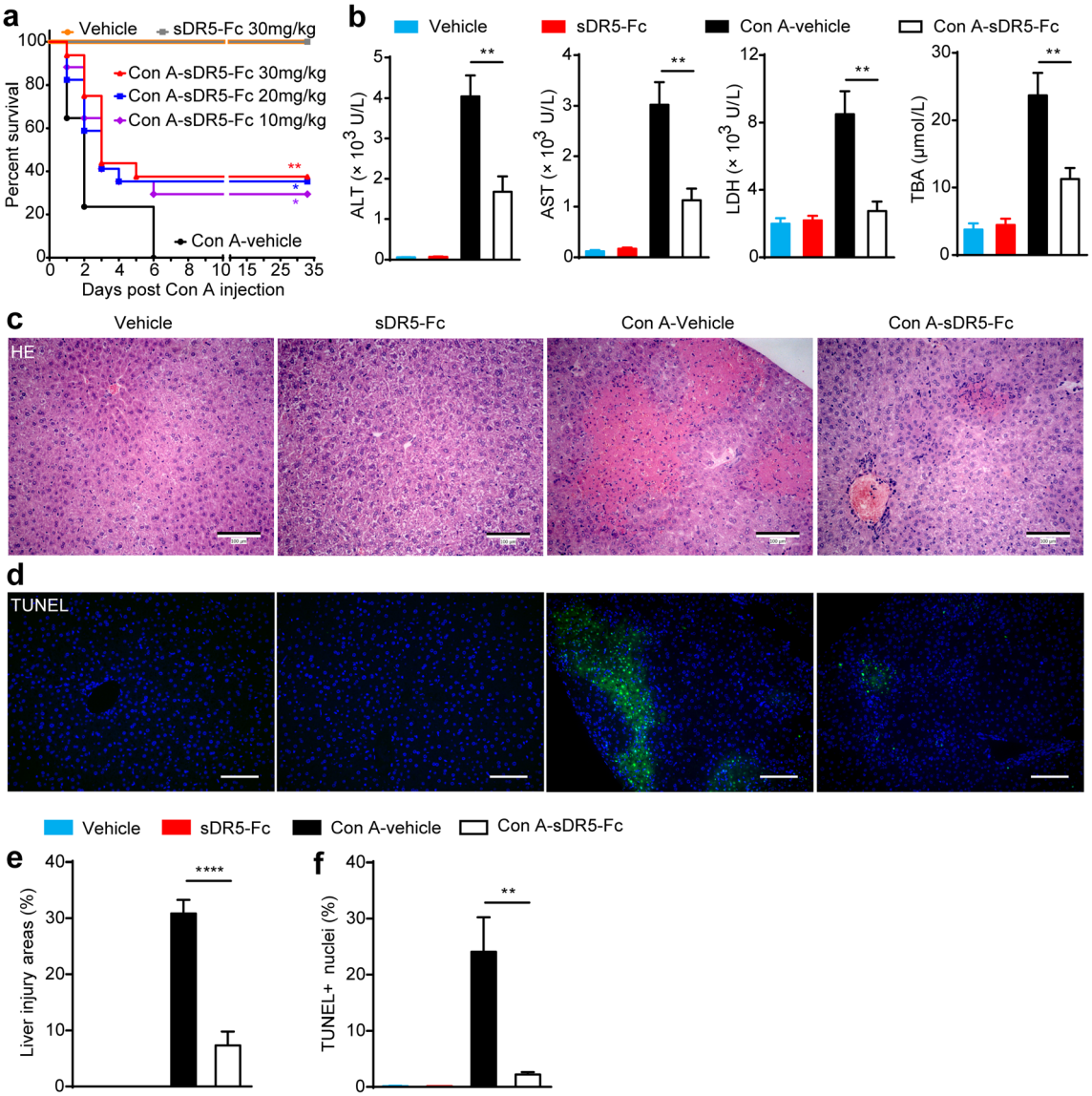

Fig. 2 sDR5-Fc protects against Con A-induced acute liver failure. **a** The survival rates of mice ($n = 10$–17 per group) challenged without or with a lethal dose of Con A (17 mg/kg, i.v.) and treated with sDR5-Fc (10–30 mg/kg) or saline (vehicle control) 1 h later. $^{*}P < 0.05$, $^{**}P < 0.01$ vs. Con A-vehicle by log-rank (Mantel-Cox) test. **b**–**e** Mice ($n = 10$ per group) were injected without or with Con A (9 mg/kg, i.v.) and then administered 9 mg/kg sDR5-Fc or the vehicle 1 h later. Blood and liver samples were harvested at 24 h after Con A injection. **b** Serum ALT, AST, LDH, and TBA levels were quantified. **c**, **e** Hepatic injury was determined by HE staining. **d**, **f** A TUNEL assay was used to evaluate apoptotic cells. Scale bars (**c**, **d**), 100 μm. The data shown in **b**, **e**, and **f** represent the mean ± SEM of one representative experiment out of three experiments. $^{**}P < 0.01$ and $^{****}P < 0.0001$ by Student's *t* test. TUNEL, terminal deoxynucleotidyl transferase-mediated deoxyuridine triphosphate (dUTP) nick end labeling

TRAIL-deficient splenocytes have reduced cytokine responses

We previously reported that hepatic cell death was dramatically reduced in TRAIL-deficient mice [18]. In this study, we found that TRAIL$^{-/-}$ mice had significantly lower serum levels of IL-6, TNF-α, and IFN-γ than TRAIL$^{+/+}$ mice after Con A injection (Fig. 5a). There was no difference in the serum IL-12 level between the TRAIL$^{-/-}$ and TRAIL$^{+/+}$ mice. To determine whether cell proliferation in response to Con A or an anti-CD3 antibody was affected by TRAIL, primary splenocytes were isolated and tested by measuring [3H]-thymidine incorporation. Compared with those from TRAIL$^{+/+}$ mice, splenocytes from TRAIL$^{-/-}$ mice demonstrated increased cell proliferation (Fig. 5b). However, the levels of IFN-γ and IL-4 in the culture supernatants of TRAIL$^{-/-}$ splenocytes were significantly lower than those in the culture supernatants of TRAIL$^{+/+}$ splenocytes after Con A or anti-CD3 antibody stimulation (Fig. 5c). These results indicated that TRAIL-deficient splenocytes had reduced cytokine responses, which was consistent with the results showing that

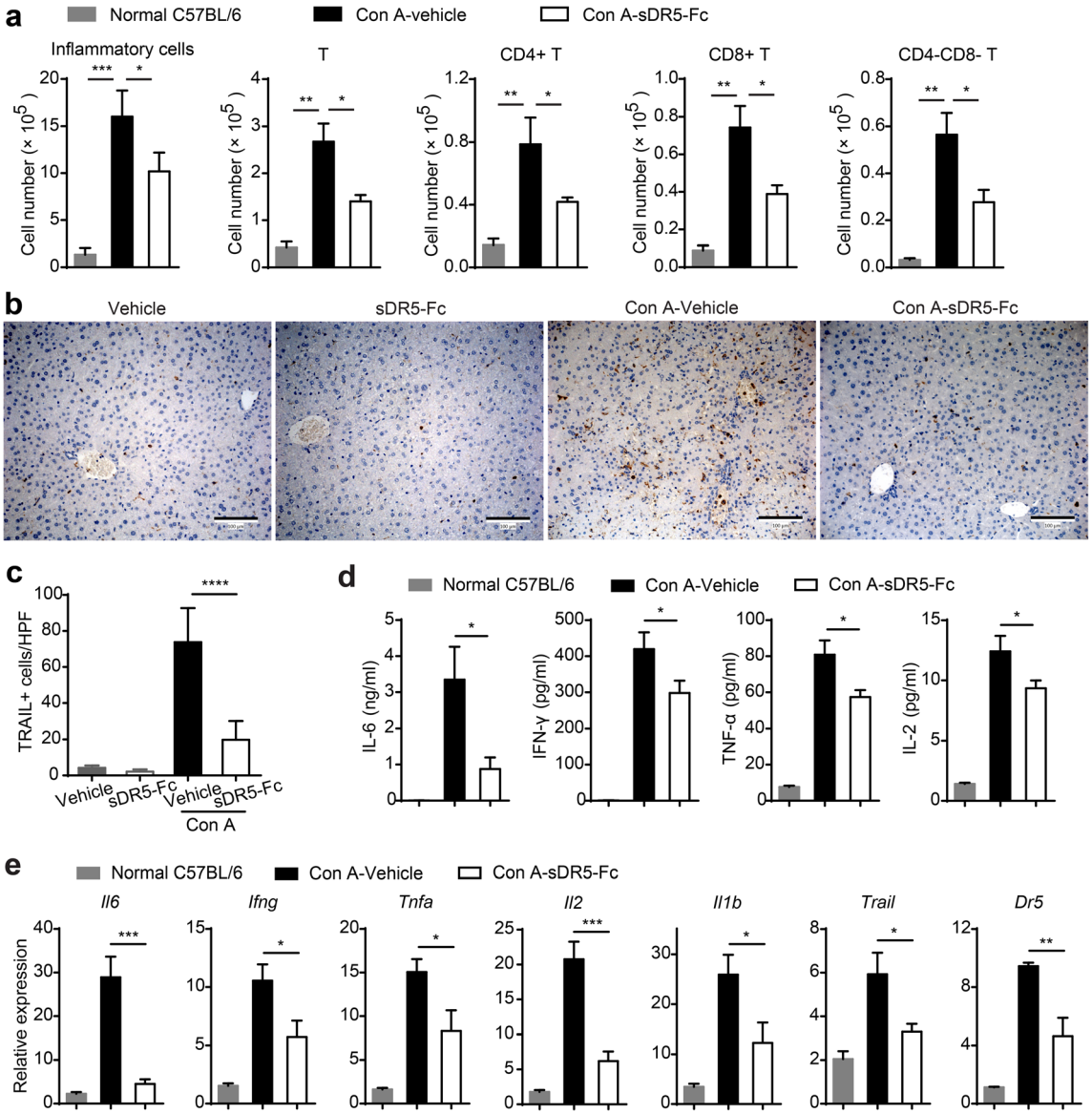

Fig. 3 sDR5-Fc attenuates the infiltration of leukocytes and the levels of inflammatory cytokines in the liver and serum during Con A-induced hepatitis in mice. Mice ($n = 6$ per group) were treated with Con A (9 mg/kg, i.v.) and then administered 9 mg/kg sDR5-Fc or the vehicle (saline) 1 h later. Livers were harvested at 8 h post-Con A injection. Liver mononuclear cells were isolated and analyzed by flow cytometry. **a** The absolute numbers of inflammatory cell populations, including T cell subsets, per gram of liver were measured. T cells, $CD45^+CD3^+CD19^-NK1.1^-$; $CD4^+$ T cells, $CD45^+CD3^+NK1.1^-CD4^+$; $CD8^+$ T cells, $CD45^+CD3^+NK1.1^-CD8^+$; and $CD4^-CD8^-$ T cells, $CD45^+CD3^+NK1.1^-CD4^-CD8^-$. **b**, **c** Liver samples were harvested at 24 h after Con A injection. Liver immunohistochemistry staining of TRAIL. HPF high-power field. Scale bars, 100 μm. **d** Serum IL-6, IFN-γ, TNF-α, and IL-2 levels at 8 h after Con A injection were detected by cytometric bead arrays. **e** Quantification of hepatic *Il6*, *Ifng*, *Tnfα*, *Il2*, *Il1b*, *Trail*, and *Dr5* mRNA expression by qPCR. All data shown are means ± SEM of one representative experiment of three. $^*P < 0.05$, $^{**}P < 0.01$, $^{***}P < 0.001$, and $^{****}P < 0.0001$ by Student's *t* test

blocking TRAIL by sDR5-Fc attenuated the production of inflammatory mediators in vitro and in vivo.

Preclinical safety studies

Before clinical trials in humans are performed, new drugs need to be extensively tested in preclinical safety studies in animals. C57BL/6 mice, Sprague-Dawley (SD) rats, and cynomolgus monkeys were used to evaluate the potential acute toxicity and long-term toxicity of the sDR5-Fc protein. There were no significant changes in body weight, coat, behavior, food consumption, secretions, feces, eyes, or respiration, and no apparent increase in lethality was observed in mice, rats, or monkeys treated with a single dose of sDR5-Fc compared to the animals treated with the vehicle (Fig. 6a–c, Supplementary Fig. S6). The anatomy of each animal was examined, and no abnormalities were observed in the major organs, including the brain, liver, spleen, kidneys, and skin. These results

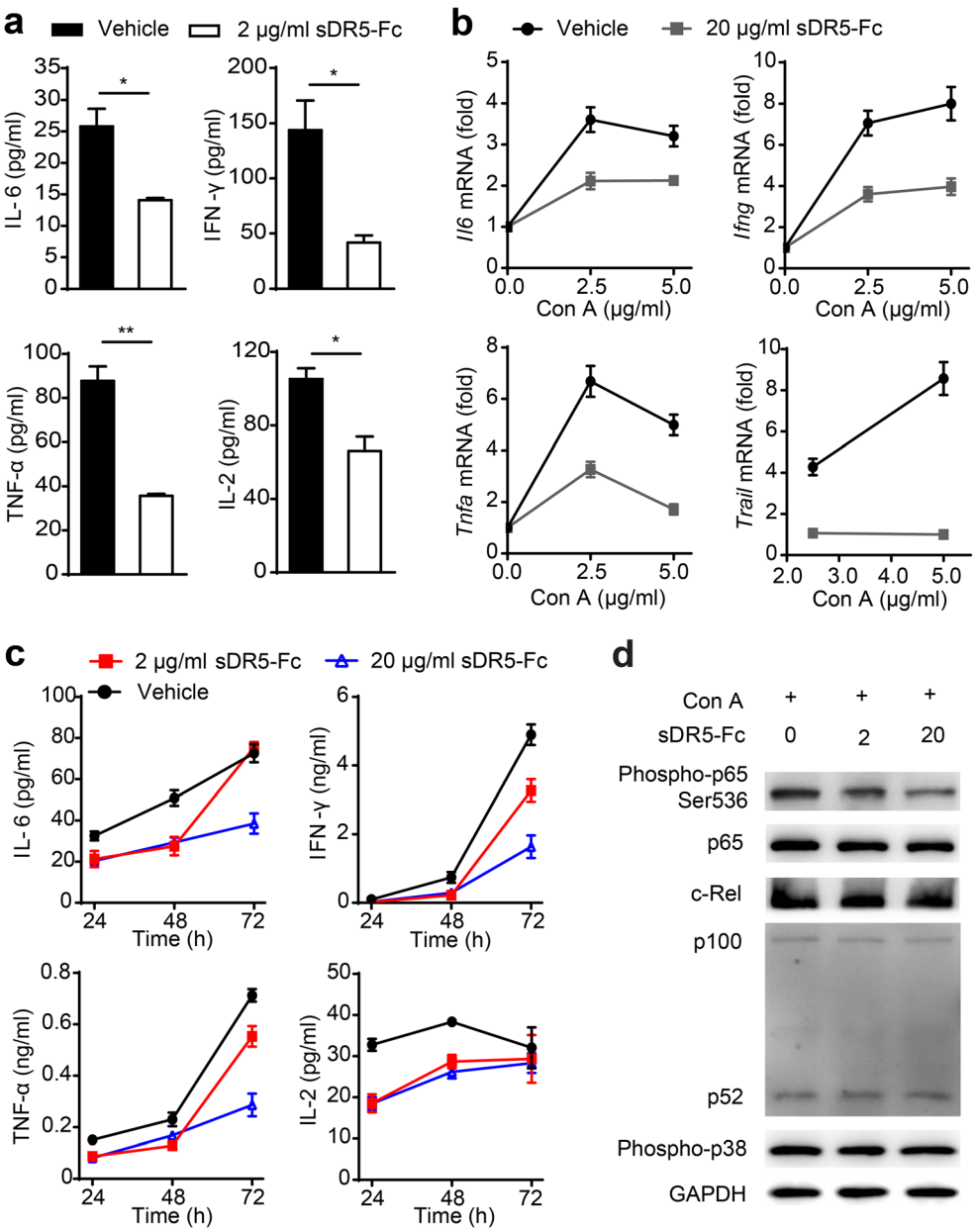

Fig. 4 sDR5-Fc inhibits the production of inflammatory mediators. Primary splenocytes were isolated from normal C57BL/6 mice and cultured. **a** IL-6, IFN-γ, TNF-α, and IL-2 concentrations in the culture supernatants of splenocytes treated with Con A (5 μg/mL) for 24 h as well as with sDR5-Fc or the vehicle, as measured by cytometric bead arrays. $*P < 0.05$ and $**P < 0.01$. **b** Quantification of *Il6*, *Ifng*, *Tnfa*, and *Trail* mRNA expression by qPCR in splenocytes treated without or with Con A (2.5 μg/mL or 5 μg/mL) for 24 h as well as with sDR5-Fc or the vehicle. **c** IL-6, IFN-γ, TNF-α, and IL-2 concentrations in the culture supernatants of splenocytes treated with an anti-CD3 antibody (1 μg/mL) and sDR5-Fc or the vehicle. All data shown are means ± SEM of one representative experiment of three. **d** Western blotting was used to analyze phospho-p65, p65, c-Rel, p100/p52, and phospho-p38 levels. Splenocytes were treated with Con A (5 μg/mL) for 24 h without or with sDR5-Fc (2 or 20 μg/mL)

suggested that the maximum tolerated doses (MTDs) of sDR5-Fc in mice, rats, and cynomolgus monkeys, when injected intravenously, were greater than 2198 mg/kg, 1500 mg/kg, and 1200 mg/kg, respectively.

In multiple-dose studies, sDR5-Fc was administered to SD rats and cynomolgus monkeys once per week for 13 weeks followed by a 4-week treatment-free phase. The intravenous injection of sDR5-Fc at high, middle, and low dosages was well tolerated in the rats and monkeys. No early deaths or no obvious signs of systemic toxicity or abnormalities were noted, and there were no test article-related effects on body weight, body temperature, or food consumption (Fig. 6d, e). No treatment-related histopathological findings were observed during the whole study period. In addition, in the monkeys, there were no detectable sDR5-Fc-related effects on the serum levels of procarcinogenic cytokines, such as epidermal growth factor (EGF), transforming growth factor (TGF-α), TGF-β, vascular endothelial growth factor (VEGF), hepatocyte growth factor (HGF), and stem cell factor (SCF) (Supplementary Fig. S7a). There were no differences in the inflammatory cytokine levels or the frequencies of T lymphocyte subsets between the vehicle- and sDR5-Fc-treated monkeys (Supplementary Fig. S7b, c). These results suggested that the no observed adverse effect level (NOAEL) of sDR5-Fc administered by repeated intravenous infusion was 200 mg/kg in SD rats and 100 mg/kg in cynomolgus monkeys, respectively.

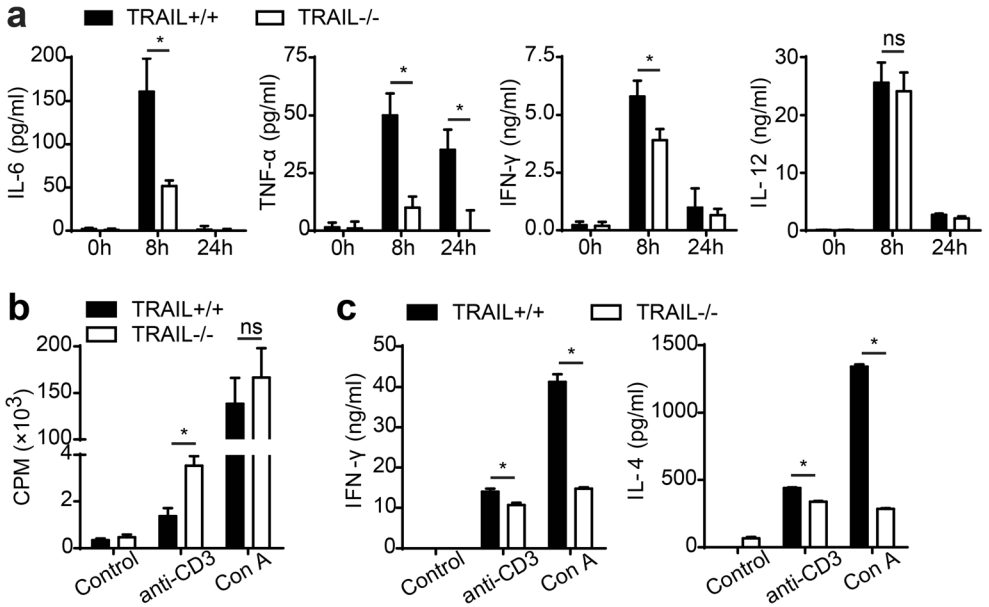

Fig. 5 TRAIL-deficient splenocytes have reduced cytokine responses. Normal ($TRAIL^{+/+}$) and TRAIL-deficient ($TRAIL^{-/-}$) mice ($n = 5$ per group) were injected with 25 mg/kg Con A. Blood was harvested at 0, 8, and 24 h after the Con A injection. **a** Serum levels of IL-6, TNF-α, IFN-γ, and IL-12 were detected by ELISA. **b**, **c** Primary splenocytes were isolated from the normal and $TRAIL^{-/-}$ mice and cultured for 72 h without or with Con A (5 μg/mL) or an anti-CD3 antibody (1 μg/mL). **b** The proliferation of the splenocytes was assessed by [3H]-thymidine incorporation and is expressed as counts per min (CPM). **c** IFN-γ and IL-4 concentrations in the culture supernatants were determined by ELISA. All data shown are means ± SD of one representative experiment of three. $^*P < 0.05$. ns, $P > 0.05$

Pharmacokinetic studies

The pharmacokinetics of sDR5-Fc were evaluated in cynomolgus monkeys as a prelude to testing in humans. The mean plasma concentration-time course curves of sDR5-Fc after a single intravenous administration or repeated intravenous administrations are shown in Fig. 6f, g, respectively. The major pharmacokinetic parameters were calculated by a noncompartmental model based on the statistical moment and are shown in Table 2. There were no obvious sex-related differences in the pharmacokinetic parameters of sDR5-Fc in the monkeys. The exposure to sDR5-Fc, as assessed by the Cmax and AUC, increased in an approximately dose-proportional manner for doses between 3 and 30 mg/kg. In addition, we evaluated the pharmacokinetics of sDR5-Fc in C57BL/6 mice (Fig. 6h, Table 2) to provide useful information for the pharmacodynamic study.

In the toxicokinetic study, sDR5-Fc was administered to cynomolgus monkeys once per week for 13 weeks followed by a 4-week recovery period. On study days 1 and 85, the exposure to sDR5-Fc increased in a dose-proportional manner across the investigated dose range (10–300 mg/kg). After 12 weekly doses, the mean accumulation ratios (based on the AUC) were 2.11, 2.11, and 1.82 for 10, 30, and 100 mg/kg sDR5-Fc, respectively, indicating that sDR5-Fc did not accumulate significantly in the animals.

Tissue distribution and excretion studies

The tissue distribution of sDR5-Fc was determined by intravenous administration of 4.2 mg/kg ^{125}I-sDR5-Fc in SD rats. The results indicated that ^{125}I-sDR5-Fc was widely distributed in rat tissues within the time course examined (Fig. 6i). The highest tissue concentration was found in the plasma at 10 min, followed by the spleen, lungs, kidneys, gonads, heart, liver, stomach, pancreas, intestine, muscle, and fat, and very little ^{125}I-sDR5-Fc was found in the brain. The ^{125}I-sDR5-Fc concentration decreased markedly at 168 h post-dosing.

Fig. 6 Safety, pharmacokinetic, tissue distribution, and excretion studies of the sDR5-Fc protein. Animals were i.v. administered sDR5-Fc or the vehicle. **a**–**c** Safety studies of a single dose of sDR5-Fc in mice (**a**, $n = 10$ per group), rats (**b**, $n = 10$ per group), and cynomolgus monkeys (**c**, $n = 6$ per group). **d**, **e** Safety studies of multiple doses of sDR5-Fc in rats (**d**, $n = 30$ per group) and cynomolgus monkeys (**e**, $n = 10$ per group). sDR5-Fc was administered once per week for 13 weeks followed by a 4-week treatment-free phase. **f** Mean (± SEM) serum concentration-time profiles of cynomolgus monkeys after the administration of a single dose of sDR5-Fc ($n = 6$ per group). **g** Mean (± SEM) serum concentration-time profiles of cynomolgus monkeys after the administration of multiple doses of sDR5-Fc ($n = 6$ per group). **h** A mean (± SEM) serum concentration-time curve of C57BL/6 mice after the administration of a single dose of 10 mg/kg sDR5-Fc ($n = 5$ per group). **i** Distribution of ^{125}I-sDR5-Fc in rats ($n = 6$ per group, 4.2 mg/kg). **j**, **k** Urine, fecal, and biliary cumulative excretion of ^{125}I-sDR5-Fc in rats ($n = 6$ per group, 4.2 mg/kg). Data shown (**a**–**e**, **j**, **k**) are means ± SD

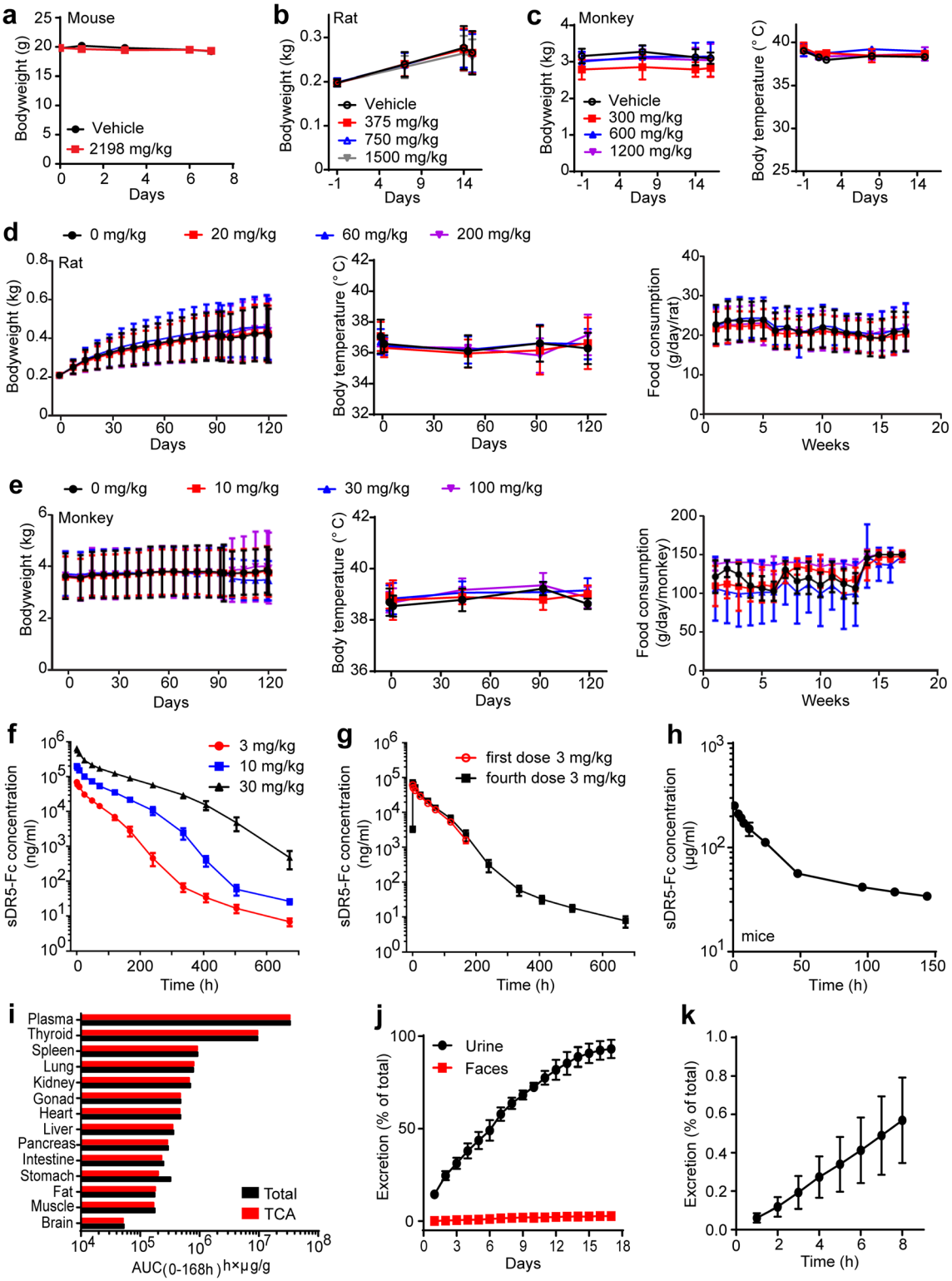

The excretion data for ^{125}I-sDR5-Fc in rat urine, feces, and bile are presented in Fig. 6j, k. Urine and fecal excretion within 17 days of sDR5-Fc administration were approximately 93.65% ± 4.94% and 3.28% ± 0.74%, respectively (Fig. 6j). Biliary excretion within 8 h was approximately 0.57% ± 0.22% (Fig. 6k). These results indicated that after a single intravenous administration, most of the ^{125}I-sDR5-Fc was excreted in the urine, with the rest excreted in the feces or bile.

Table 2 The mean noncompartmental pharmacokinetic parameters of sDR5-Fc after intravenous administration

Species		Cynomolgus monkey[a]					Mouse[b]
Dose (mg/kg)		Single dose			Multiple dose		Single dose
					First	Fourth	
		3	10	30	3	3	10
$t_{1/2}$ (h)	Mean	103.45	46.44	47.25	34.11	87.34	55.09
	SD	14.96	7.28	9.79	5.92	47.90	2.60
C_{max} (μg/mL)	Mean	68.62	200.51	638.72	60.88	72.14	386.8
	SD	8.10	31.27	91.94	10.28	6.15	184.2
AUC_{last} (h mg/mL)	Mean	3.05	12.37	45.35	2.49	3.09	13.79
	SD	0.60	3.40	6.95	0.42	0.68	2.11
AUC_{inf} (h mg/mL)	Mean	3.05	12.37	45.39	2.58	3.09	16.16
	SD	0.60	3.41	7.00	0.46	0.68	1.78
V (mL/kg)	Mean	150.97	56.34	45.30	57.80	117.68	50.00
	SD	33.62	11.05	7.75	8.73	49.93	5.95
CL (mL/h/kg)	Mean	1.02	0.87	0.67	1.20	1.01	0.63
	SD	0.20	0.29	0.10	0.23	0.22	0.07
MRT (h)	Mean	51.70	78.52	114.65	42.86	48.10	51.55
	SD	10.42	14.94	24.33	4.90	12.41	2.46
$AUC_{(0–168\ h)}$ (h mg/mL)	Mean	2.89	10.43	32.87	2.49	2.97	NA
	SD	0.48	2.33	2.57	0.42	0.59	NA

$t_{1/2}$, half-life time; C_{max}, maximum observed concentration for i.v. dosing; AUC_{last}, AUC_{inf}, $AUC_{(0–168\ h)}$, areas under the curve from 0 h to the end of observation, 0 to ∞ h, and 0 to 168 h, respectively; *V*, volume of distribution at the terminal phase; *CL*, clearance; *MRT*, mean residence time extrapolated to infinity; *NA*, not available

[a] $n = 6$ per group

[b] $n = 5$ per group

Discussion

In this study, we expressed and purified a recombinant human sDR5-Fc fusion protein and tested it in preclinical studies in three species of animals. The results showed that sDR5-Fc was a suitable drug candidate for blocking TRAIL-mediated pathologies. Naturally occurring sDR5 consists of 138 amino acids and has a predicted molecular mass of 15.8 kDa. It is well recognized that peptides and proteins smaller than 70 kDa can be eliminated via kidney filtration; thus, they generally possess very short serum half-lives. To extend the half-life of sDR5, an sDR5-Fc fusion protein was created in this study. Due to glycosylation and dimerization, the apparent molecular mass of sDR5-Fc was 79.4 kDa, and linear pharmacokinetics with a half-life between 1.9 and 4.3 days were observed in cynomolgus monkeys after a single dose.

The amino acid sequence of the functional extracellular domain of rhesus monkey TRAIL has been found to differ from that of human TRAIL at only four positions; therefore, monkey TRAIL and human TRAIL have comparable affinities for human death receptors [33]. Consistent with these results, we found that the affinity of human sDR5-Fc for human TRAIL was comparable to that for monkey TRAIL, which supports the use of cynomolgus monkeys as a relevant toxicology model for this fusion protein. Murine TRAIL is 65% identical to human TRAIL [34], human sDR5 shares 79% sequence homology with murine sDR5, and recombinant human sDR5 effectively blocks murine TRAIL [35]. Similarly, our sDR5-Fc protein could bind with mouse TRAIL and was highly efficacious in a mouse ALF model.

Of note, we found that the EC_{50} values of sDR5-Fc for blocking TRAIL in L929, HepG2, and Jurkat cells were in the pM to nM range, and the affinity of sDR5-Fc binding to human TRAIL was in the nM range, which were consistent with previous results [36]. In addition to binding with its ligand, sDR5 has been reported to interact homophilically or heterophilically with micromolar range affinities (K_D), e.g., ~ 2.2 μM for sDR5-sDR5 and ~ 8.1 μM for sDR5-sDR4 [36]. Vunnam et al. also found that sDR5 can interact with membrane-bound DR5 in a dose-dependent manner, with an EC_{50} of ~ 4.6 μM (78.2 μg/mL) [30]. By disrupting receptor-receptor interactions, sDR5 can inhibit TRAIL-induced apoptosis [30]. However, we did not detect clear binding interactions between sDR5-Fc (up to 100 μg/mL) and membrane-bound DR5 in L929 or HepG2 cells, which could be due to the decreased sensitivity of the detection method compared to

fluorescence resonance energy transfer (FRET), or the low expression level of membrane-bound DR5 in these cells compared to that in the HEK293 cells stably transfected with DR5 expression plasmids used by Vunnam et al. Our results confirmed that sDR5-Fc had obviously higher binding affinity for TRAIL than for sDR5. Based on these results, the effective concentration of sDR5 needed for receptor-receptor interaction is approximately 3~4 orders of magnitude higher than that needed for receptor-ligand interaction. Thus, the antiapoptotic effect of sDR5-Fc should be mainly due to the sequestration of TRAIL. Under physiological conditions, sDR5-Fc binding to TRAIL should be favored, especially when there is a low concentration of sDR5-Fc.

In the Con A model, mice develop acute, partly apoptotic hepatic injury that is subsequently overlaid by massive necrosis [22, 37], and cytotoxic effector molecules and their receptors, such as TRAIL/DR5, TNF-α/TNFR, FasL/Fas, and perforin-granzyme, play crucial roles in hepatitis development and hepatocyte death [18, 38–40]. Our data demonstrated that sDR5-Fc was specific for TRAIL and did not directly interact with TNF-α or FasL (Supplementary Fig. S8a-c). TRAIL is a well-known inducer of apoptosis. We found that Con A induced sTRAIL in the mouse serum and that the sTRAIL level correlated with the severity of ALF (Supplementary Fig. S8d). Treatment with sDR5-Fc reduced the number of apoptotic hepatocytes in Con A-treated mice. In addition, it should be noted that the major mode of hepatic cell death induced by Con A is necrosis rather than apoptosis [41]. We did not observe many cleaved caspase-3-positive hepatocytes in the Con A-injected mice (Supplementary Fig. S8e), which is in line with the aforementioned reports [38, 42]. Furthermore, the pancaspase inhibitor z-VAD does not affect the level of ALT in response to Con A [43]. Therefore, we believe that the major therapeutic effect of sDR5-Fc in Con A-induced ALF is not only dependent on directly inhibiting TRAIL-induced hepatocyte apoptosis.

Apart from inducing apoptosis, TRAIL stimulation can result in the activation of NF-κB and the production of inflammatory cytokines and chemokines [44]. We found that Con A induced the infiltration of TRAIL-expressing inflammatory cells into the liver and the expression of high levels of proinflammatory cytokines. Treatment with sDR5-Fc attenuated inflammation in vivo, including decreasing hepatic proinflammatory cytokine mRNA levels and serum cytokine levels. Mechanistically, we observed that blocking TRAIL with sDR5-Fc attenuated the production of inflammatory mediators by Con A-activated splenocytes in vitro by inhibiting activation of the transcription factor NF-κB. Upon stimulation with Con A, $TRAIL^{-/-}$ mice produced markedly less IL-6, TNF-α, and IFN-γ than $TRAIL^{+/+}$ mice, which was in line with the action of sDR5-Fc. Therefore, the evidence presented in this study established that the mechanism underlying the therapeutic effect of sDR5-Fc on Con A-induced ALF involves sDR5-Fc directly binding with TRAIL to inhibit the activation of NF-κB and inflammation.

Approximately 25% of $TRAIL^{-/-}$ mice develop lymphoid malignancies after 500 days of life, and TRAIL has been shown to suppress the initiation and development of tumors [45], which raises questions regarding the safety of sDR5-Fc, a TRAIL blocker. In cynomolgus monkeys, the MTD of sDR5-Fc administered in a single i.v. infusion exceeded 1200 mg/kg, and once weekly i.v. administration of sDR5-Fc for up to 13 weeks was well tolerated at a dose of up to 100 mg/kg. In addition, there were no detectable sDR5-Fc-related effects on the procarcinogenic cytokines, inflammatory cytokines, or the frequencies of T lymphocyte subsets in the monkeys treated with repeated doses over 13 weeks. Furthermore, no significant accumulation of sDR5-Fc was found. These findings indicated the safety of sDR5-Fc in treating ALF.

Con A-induced hepatitis in mice is an experimental model of T cell-mediated liver injury and liver failure that resembles viral or autoimmune liver disease in humans [22, 31]. Studies with other animal models have shown that interrupting TRAIL signaling ameliorates acute liver injury following HBV transfection [19], cholestatic liver injury and fibrogenesis in the bile duct-ligated animals [46, 47], *Listeria*-induced hepatitis [18], and steatohepatitis following saturated fat, cholesterol, and fructose use [48]. Therefore, additional studies are needed to evaluate the therapeutic efficacy of sDR5-Fc in these diseases in the future.

In conclusion, our work demonstrates that sDR5-Fc, which has the potential to be the first TRAIL-blocking therapeutic drug, holds great promise for future clinical development and testing in humans for the treatment of TRAIL-driven diseases.

Acknowledgments We thank Lihong Qin and Shengrong Li at Amshenn Inc. for technical and administrative support; Drs. Yajun Guo, Hao Wang, Jing Li, and their team of scientists at Shanghai Zhangjiang Biotech for technical support and valuable discussions regarding the design and manufacturing of the sDR5-Fc protein. We gratefully acknowledge the technical support provided by scientists at JOINN Inc. for the preclinical safety and pharmacokinetic studies of sDR5-Fc.

Author contributions Q.C., P.W., Q.Z., and M.X. performed the experimental work and analyzed the data. Y.C. and X.W. supervised the design of the experiments. G.Z., J.L., and E.S. provided other essential tools and useful comments and suggestions. Q.C. and Y.C. wrote the manuscript.

Funding information This work was partially supported by the fourth talents project of Guangdong province (2014-1), special funds for major science and technology of Guangdong province (2013A022100037), Shenzhen peacock team project (1110140040347265), Shenzhen Science and Technology Program (Grant Nos. JSGG20160229202150023, JCYJ20170818164619194, and JCYJ20170413153158716), and Nanshan pilot team project (LHTD20160001). This work was also supported by Shenzhen special funds for industry of the future (2015-971).

Compliance with ethical standards

Ethical approval All applicable international, national, and/or institutional guidelines for the care and use of animals were followed. The manuscript does not contain clinical studies or patient data.

Conflict of interest X.W. and Y.C. are members of the advisory board of Amshenn Co. The other authors declare that they have no conflict of interest.

References

1. Punzalan CS, Barry CT (2016) Acute liver failure: diagnosis and management. J Intensive Care Med 31(10):642–653
2. McPhail MJ, Kriese S, Heneghan MA (2015) Current management of acute liver failure. Curr Opin Gastroenterol 31(3):209–214
3. Canbay A, Friedman S, Gores GJ (2004) Apoptosis: the nexus of liver injury and fibrosis. Hepatology 39(2):273–278
4. Schneider P, Thome M, Burns K, Bodmer JL, Hofmann K, Kataoka T, Holler N, Tschopp J (1997) TRAIL receptors 1 (DR4) and 2 (DR5) signal FADD-dependent apoptosis and activate NF-kappaB. Immunity 7(6):831–836
5. Saitou Y, Shiraki K, Fuke H, Inoue T, Miyashita K, Yamanaka Y, Yamaguchi Y, Yamamoto N, Ito K, Sugimoto K, Nakano T (2005) Involvement of tumor necrosis factor-related apoptosis-inducing ligand and tumor necrosis factor-related apoptosis-inducing ligand receptors in viral hepatic diseases. Hum Pathol 36(10):1066–1073
6. Mundt B, Kuhnel F, Zender L, Paul Y, Tillmann H, Trautwein C, Manns MP, Kubicka S (2003) Involvement of TRAIL and its receptors in viral hepatitis. FASEB J 17(1):94–96
7. Strater J, Moller P (2004) TRAIL and viral infection. Vitam Horm 67:257–274
8. Maini MK, Peppa D (2013) NK cells: a double-edged sword in chronic hepatitis B virus infection. Front Immunol 4:57. https://doi.org/10.3389/fimmu.2013.00057
9. Han LH, Sun WS, Ma CH, Zhang LN, Liu SX, Zhang Q, Gao LF, Chen YH (2002) Detection of soluble TRAIL in HBV infected patients and its clinical implications. World J Gastroenterol 8(6):1077–1080
10. Dunn C, Brunetto M, Reynolds G, Christophides T, Kennedy PT, Lampertico P, Das A, Lopes AR, Borrow P, Williams K, Humphreys E, Afford S, Adams DH, Bertoletti A, Maini MK (2007) Cytokines induced during chronic hepatitis B virus infection promote a pathway for NK cell-mediated liver damage. J Exp Med 204(3):667–680
11. Malhi H, Barreyro FJ, Isomoto H, Bronk SF, Gores GJ (2007) Free fatty acids sensitise hepatocytes to TRAIL mediated cytotoxicity. Gut 56(8):1124–1131
12. Higuchi H, Bronk SF, Taniai M, Canbay A, Gores GJ (2002) Cholestasis increases tumor necrosis factor-related apoptotis-inducing ligand (TRAIL)-R2/DR5 expression and sensitizes the liver to TRAIL-mediated cytotoxicity. J Pharmacol Exp Ther 303(2):461–467
13. Song CJ, Liu XS, Zhu Y, Chen LH, Jia W, Li YN, Cao YX, Xie X, Zhuang R, Zhu CS, Jin BQ (2004) Expression of TRAIL, DR4, and DR5 in kidney and serum from patients receiving renal transplantation. Transplant Proc 36(5):1340–1343
14. Komatsuda A, Wakui H, Iwamoto K, Togashi M, Maki N, Masai R, Hatakeyama T, Sawada K (2007) Up-regulation of TRAIL mRNA expression in peripheral blood mononuclear cells from patients with active systemic lupus erythematosus. Clin Immunol 125(1):26–29
15. Walczak H, Degli-Esposti MA, Johnson RS, Smolak PJ, Waugh JY, Boiani N, Timour MS, Gerhart MJ, Schooley KA, Smith CA, Goodwin RG, Rauch CT (1997) TRAIL-R2: a novel apoptosis-mediating receptor for TRAIL. EMBO J 16(17):5386–5397
16. Song K, Chen Y, Goke R, Wilmen A, Seidel C, Goke A, Hilliard B, Chen Y (2000) Tumor necrosis factor-related apoptosis-inducing ligand (TRAIL) is an inhibitor of autoimmune inflammation and cell cycle progression. J Exp Med 191(7):1095–1104
17. Zhang HG, Xie J, Xu L, Yang P, Xu X, Sun S, Wang Y, Curiel DT, Hsu HC, Mountz JD (2002) Hepatic DR5 induces apoptosis and limits adenovirus gene therapy product expression in the liver. J Virol 76(11):5692–5700
18. Zheng SJ, Wang P, Tsabary G, Chen YH (2004) Critical roles of TRAIL in hepatic cell death and hepatic inflammation. J Clin Invest 113(1):58–64
19. Liu YG, Liu SX, Liang XH, Zhang Q, Gao LF, Han LH, Cao YL, Hou N, Du J, Sun WS (2007) Blockade of TRAIL pathway ameliorates HBV-induced hepatocyte apoptosis in an acute hepatitis model. Biochem Biophys Res Commun 352(2):329–334
20. Kilkenny C, Browne W, Cuthill IC, Emerson M, Altman DG, Group NCRRGW (2010) Animal research: reporting in vivo experiments: the ARRIVE guidelines. J Gene Med 12(7):561–563
21. McGrath JC, Lilley E (2015) Implementing guidelines on reporting research using animals (ARRIVE etc.): new requirements for publication in BJP. Br J Pharmacol 172(13):3189–3193
22. Tiegs G, Hentschel J, Wendel A (1992) A T cell-dependent experimental liver injury in mice inducible by concanavalin A. J Clin Invest 90(1):196–203
23. Santodomingo-Garzon T, Swain MG (2011) Role of NKT cells in autoimmune liver disease. Autoimmun Rev 10(12):793–800
24. Wang HX, Liu M, Weng SY, Li JJ, Xie C, He HL, Guan W, Yuan YS, Gao J (2012) Immune mechanisms of concanavalin A model of autoimmune hepatitis. World J Gastroenterol 18(2):119–125
25. Sass G, Heinlein S, Agli A, Bang R, Schumann J, Tiegs G (2002) Cytokine expression in three mouse models of experimental hepatitis. Cytokine 19(3):115–120
26. Lamhamedi-Cherradi SE, Zheng SJ, Maguschak KA, Peschon J, Chen YH (2003) Defective thymocyte apoptosis and accelerated autoimmune diseases in TRAIL−/− mice. Nat Immunol 4(3):255–260
27. Wang J, Sun R, Wei H, Dong Z, Gao B, Tian Z (2006) Poly I:C prevents T cell-mediated hepatitis via an NK-dependent mechanism. J Hepatol 44(3):446–454
28. Lu X, Fu H, Han F, Fang Y, Xu J, Zhang L, Du Q (2018) Lipoxin A4 regulates PM2.5-induced severe allergic asthma in mice via the Th1/Th2 balance of group 2 innate lymphoid cells. J Thorac Dis 10(3):1449–1459
29. Livak KJ, Schmittgen TD (2001) Analysis of relative gene expression data using real-time quantitative PCR and the 2(−Delta Delta C(T)) method. Methods 25(4):402–408
30. Vunnam N, Lo CH, Grant BD, Thomas DD, Sachs JN (2017) Soluble extracellular domain of death receptor 5 inhibits TRAIL-induced apoptosis by disrupting receptor-receptor interactions. J Mol Biol 429(19):2943–2953
31. Takeda K, Hayakawa Y, Van Kaer L, Matsuda H, Yagita H, Okumura K (2000) Critical contribution of liver natural killer T cells to a murine model of hepatitis. Proc Natl Acad Sci U S A 97(10):5498–5503
32. Diao W, Jin F, Wang B, Zhang CY, Chen J, Zen K, Li L (2014) The protective role of myeloid-derived suppressor cells in concanavalin A-induced hepatic injury. Protein Cell 5(9):714–724
33. Jia D, Yang H, Tao Z, Wan L, Cheng J, Lu X (2016) Preparation and characterization of a novel variant of human tumor necrosis factor-related apoptosis-inducing ligand from the rhesus monkey, Macaca mulatta. Appl Microbiol Biotechnol 100(7):3035–3047
34. Wiley SR, Schooley K, Smolak PJ, Din WS, Huang CP, Nicholl JK, Sutherland GR, Smith TD, Rauch C, Smith CA, Goodwin RG

(1995) Identification and characterization of a new member of the TNF family that induces apoptosis. Immunity 3(6):673–682
35. Schneider P, Olson D, Tardivel A, Browning B, Lugovskoy A, Gong D, Dobles M, Hertig S, Hofmann K, Van Vlijmen H, Hsu YM, Burkly LC, Tschopp J, Zheng TS (2003) Identification of a new murine tumor necrosis factor receptor locus that contains two novel murine receptors for tumor necrosis factor-related apoptosis-inducing ligand (TRAIL). J Biol Chem 278(7):5444–5454
36. Lee HW, Lee SH, Lee HW, Ryu YW, Kwon MH, Kim YS (2005) Homomeric and heteromeric interactions of the extracellular domains of death receptors and death decoy receptors. Biochem Biophys Res Commun 330(4):1205–1212
37. Gantner F, Leist M, Lohse AW, Germann PG, Tiegs G (1995) Concanavalin A-induced T-cell-mediated hepatic injury in mice: the role of tumor necrosis factor. Hepatology 21(1):190–198
38. Kunstle G, Hentze H, Germann PG, Tiegs G, Meergans T, Wendel A (1999) Concanavalin A hepatotoxicity in mice: tumor necrosis factor-mediated organ failure independent of caspase-3-like protease activation. Hepatology 30(5):1241–1251
39. Kovalovich K, Li W, DeAngelis R, Greenbaum LE, Ciliberto G, Taub R (2001) Interleukin-6 protects against Fas-mediated death by establishing a critical level of anti-apoptotic hepatic proteins FLIP, Bcl-2, and Bcl-xL. J Biol Chem 276(28):26605–26613
40. Beraza N, Malato Y, Sander LE, Al-Masaoudi M, Freimuth J, Riethmacher D, Gores GJ, Roskams T, Liedtke C, Trautwein C (2009) Hepatocyte-specific NEMO deletion promotes NK/NKT cell- and TRAIL-dependent liver damage. J Exp Med 206(8): 1727–1737
41. Jouan-Lanhouet S, Arshad MI, Piquet-Pellorce C, Martin-Chouly C, Le Moigne-Muller G, Van Herreweghe F, Takahashi N, Sergent O, Lagadic-Gossmann D, Vandenabeele P, Samson M, Dimanche-Boitrel MT (2012) TRAIL induces necroptosis involving RIPK1/RIPK3-dependent PARP-1 activation. Cell Death Differ 19(12): 2003–2014
42. Wroblewski R, Armaka M, Kondylis V, Pasparakis M, Walczak H, Mittrucker HW, Schramm C, Lohse AW, Kollias G, Ehlken H (2016) Opposing role of tumor necrosis factor receptor 1 signaling in T cell-mediated hepatitis and bacterial infection in mice. Hepatology 64(2):508–521
43. Schattenberg JM, Zimmermann T, Worns M, Sprinzl MF, Kreft A, Kohl T, Nagel M, Siebler J, Schulze Bergkamen H, He YW, Galle PR, Schuchmann M (2011) Ablation of c-FLIP in hepatocytes enhances death-receptor mediated apoptosis and toxic liver injury in vivo. J Hepatol 55(6):1272–1280
44. Berg D, Stuhmer T, Siegmund D, Muller N, Giner T, Dittrich-Breiholz O, Kracht M, Bargou R, Wajant H (2009) Oligomerized tumor necrosis factor-related apoptosis inducing ligand strongly induces cell death in myeloma cells, but also activates proinflammatory signaling pathways. FEBS J 276(23):6912–6927
45. Zerafa N, Westwood JA, Cretney E, Mitchell S, Waring P, Iezzi M, Smyth MJ (2005) Cutting edge: TRAIL deficiency accelerates hematological malignancies. J Immunol 175(9):5586–5590
46. Kahraman A, Barreyro FJ, Bronk SF, Werneburg NW, Mott JL, Akazawa Y, Masuoka HC, Howe CL, Gores GJ (2008) TRAIL mediates liver injury by the innate immune system in the bile duct-ligated mouse. Hepatology 47(4):1317–1330
47. Fernandez-Alvarez S, Gutierrez-de Juan V, Zubiete-Franco I, Barbier-Torres L, Lahoz A, Pares A, Luka Z, Wagner C, Lu SC, Mato JM, Martinez-Chantar ML, Beraza N (2015) TRAIL-producing NK cells contribute to liver injury and related fibrogenesis in the context of GNMT deficiency. Lab Investig 95(2):223–236
48. Idrissova L, Malhi H, Werneburg NW, LeBrasseur NK, Bronk SF, Fingas C, Tchkonia T, Pirtskhalava T, White TA, Stout MB, Hirsova P, Krishnan A, Liedtke C, Trautwein C, Finnberg N, El-Deiry WS, Kirkland JL, Gores GJ (2015) TRAIL receptor deletion in mice suppresses the inflammation of nutrient excess. J Hepatol 62(5):1156–1163